Commun. Theor. Phys. **76** (2024) 075401 (9pp) https://doi.org/10.1088/1572-9494/ad426e

Restoring cosmological concordance with axion-like early dark energy and dark matter characterized by a constant equation of state?

Yan-Hong Yao[1] **and Xin-He Meng**[2]

[1] School of Physics and Astronomy, Sun Yat-sen University 2 Daxue Road, Tangjia, Zhuhai, China
[2] School of Physics, Nankai University 94 Weijin Road, Nankai, Tianjin, China

E-mail: yaoyh29@mail.sysu.edu.cn

Received 17 March 2024, revised 17 April 2024
Accepted for publication 24 April 2024
Published 12 June 2024

Abstract

The Hubble tension persists as a challenge in cosmology. Even early dark energy (EDE) models, initially considered the most promising for alleviating the Hubble tension, fall short of addressing the issue without exacerbating other tensions, such as the S_8 tension. Considering that a negative dark matter (DM) equation of state (EoS) parameter is conducive to reduce the value of the σ_8 parameter, we extend the axion-like EDE model in this paper by replacing the cold dark matter (CDM) with DM characterized by a constant EoS $w_{\rm dm}$ (referred to as WDM hereafter). We then impose constraints on this axion-like EDE extension model, along with three other models: the axion-like EDE model, ΛWDM, and ΛCDM. These constraints are derived from a comprehensive analysis incorporating data from the Planck 2018 cosmic microwave background, baryon acoustic oscillations, and the Pantheon compilation, as well as a prior on H_0 (i.e. $H_0 = 73.04 \pm 1.04$, based on the latest local measurement by Riess *et al*) and a Gaussianized prior on S_8 (i.e. $S_8 = 0.766 \pm 0.017$, determined through the joint analysis of KID1000+BOSS +2dLenS). We find that although the new model maintains the ability to alleviate the Hubble tension to $\sim 1.4\sigma$, it still exacerbates the S_8 tension to a level similar to that of the axion-like EDE model.

Keywords: Hubble tension, early dark energy, noncold dark matter, S8 tension

(Some figures may appear in colour only in the online journal)

1. Introduction

Although scrutinized by a plethora of observational data across various scales in the past, the Lambda cold dark matter (ΛCDM) model is currently facing skepticism regarding its internal inconsistencies. The Hubble tension, i.e. disagreement between direct [1] and indirect measurements [2] of the Hubble constant H_0, is a major factor contributing to this outcome. Although, up to this point, we cannot exclude the possibility of systematics as the origin of the Hubble tension, many cosmologists are beginning to address the tension by introducing new physics. Generally speaking, solutions for resolving the Hubble tension in a theoretical manner can be categorized into two types: early-time solutions and late-time solutions, based on the introduction of new physics before and after recombination. Early-time solutions, such as early dark energy (EDE) models [3–12], which introduce an exotic dark sector that acts as a cosmological constant before a critical redshift z_c around 3000 but whose density then dilutes faster than radiation, and dark radiation models [13–18], which include extra relativistic degrees of freedom that do not interact with photons and baryons, are considered to play a important role in resolving the Hubble tension. Nevertheless, as pointed out in [19], early-time new physics alone will always fall short of fully solving the Hubble tension. On the other hand, late-time solutions, such as late dark energy (DE)

models [20–26] and interacting DE models [27–39], are also considered to be incapable of fully resolving the Hubble tension, since consistency with baryon acoustic oscillation (BAO) and uncalibrated Type Ia supernovae (SN Ia) data requires new physics to be introduced before recombination, in order to reduce the sound horizon by ∼7% [40–44].

Among all the early-time solutions, EDE models may be the most promising category. However, similar to other early-time solutions, EDE models are incapable of fully resolving the Hubble tension. One of the primary reasons for this is that consideration of a non-zero EDE fraction $f_{\rm EDE}(z_c)$ near the matter–radiation equality would increase the dark matter (DM) density $\omega_{\rm cdm}$ compared to that of ΛCDM. A higher value of $\omega_{\rm cdm}$ would lead to a higher value of the $S_8 = \sigma_8\sqrt{\Omega_{\rm m}/0.3}$ parameter (where $\Omega_{\rm m}$ is the matter density parameter and σ_8 is the matter fluctuation amplitude on scales of $8h^{-1}$Mpc) if the value of σ_8 undergoes little variation, leading to a more significant S_8 tension between cosmic microwave background (CMB) data and weak lensing (WL) as well as large-scale structure (LSS) data [45–62]. However, it is still possible that an extension of an EDE model would mitigate the need for an increase in the $\omega_{\rm cdm}$ or, alternatively, compensate the associated increase in the amplitude of fluctuations. In fact, various extensions of EDE models have been proposed by researchers guided by this idea to simultaneously alleviate the H_0 tension and the S_8 tension. See e.g. [63–70]. These models employ various methods to supplement or modify the CDM paradigm, including the introduction of the total neutrino mass M_ν as a free parameter [63, 65, 70], the inclusion of ultra-light axions that comprise five percent of DM [64], the proposal to replace CDM with decaying DM [69] and the consideration of DM coupled with EDE [66–68]. Since the nature of DM remains mysterious, it is appropriate to explore phenomenological models and observe how they align with data. The simplest phenomenological modification to the CDM paradigm, i.e. considering a constant DM equation of state (EoS) as a free parameter, has not yet been explored in the existing literature related to the extension of EDE. Nevertheless, it is well known that a negative value of DM EoS has the capability to reduce the value of the σ_8 parameter compared to a CDM setting. Therefore, in this paper, we will extend the axion-like EDE model by replacing CDM with DM characterized by a constant EoS (referred to as WDM hereafter), and examine whether this extension can simultaneously alleviate the H_0 tension and the S_8 tension.

The rest of this paper is organized as follows. In section 2, we review the dynamics of axion-like EDE and WDM, and discuss their cosmological implications, specifically on the CMB and matter power spectra. In section 3, we describe the observational datasets and the statistical methodology. In section 4, we present the results of a Markov Chain Monte Carlo analysis applied on a combination of CMB, BAO and SN Ia data. In the last section, we present a brief conclusion for this paper.

2. Model overview

Our model consists of two modifications to ΛCDM. The first is the inclusion of the axion-like EDE, and the second is the replacement of CDM with WDM. Therefore, we refer to this model as EDE+WDM hereafter. In this section, we will give a brief summary of the dynamics of EDE+WDM.

In EDE+WDM, EDE is represented by a canonical scalar field [7], while WDM is represented by an ideal fluid. Their energy density and pressure affect the dynamics of other species through Einstein's equation. At the homogeneous and isotropic level, the expansion rate of the Universe can be written as:

$$H = H_0\sqrt{\Omega_{\rm dm}(a) + \Omega_b(a) + \Omega_r(a) + \Omega_\Lambda + \Omega_\phi(a)}\,, \quad (2.1)$$

where a is the scale factor, $\Omega_X \equiv \rho_X/\rho_{\rm crit}$ and $\rho_{\rm crit} = 3H_0^2M_P^2$, with $M_P \equiv (8\pi G)^{-\frac{1}{2}}$ being the reduced Planck mass. The energy density and pressure of the scalar field at the background level are given by:

$$\rho_\phi = \frac{1}{2}\dot\phi^2 + V(\phi), \quad (2.2)$$

$$p_\phi = \frac{1}{2}\dot\phi^2 - V(\phi), \quad (2.3)$$

where the dot indicates a derivative with respect to cosmic time. The potential of the axion-like EDE scalar field is chosen in the following form:

$$V(\phi) = m^2f^2\left[1 - \cos(\phi/f)\right]^3, \quad (2.4)$$

where m and f are the EDE mass and decay constant. The evolution of the scalar field ϕ is described by the Klein–Gordon (KG) equation:

$$\ddot\phi + 3H\dot\phi + V_{,\phi} = 0. \quad (2.5)$$

As described in the literature [7], initially, the scalar field is frozen due to Hubble friction at a position displaced from the minimum of its potential, and its energy density is subdominant. It is only after the Hubble rate drops below the effective mass of the scalar field that the field becomes dynamical, starts rolling down and oscillates around the minimum of its potential. This leads to a faster dilution of its energy density compared to radiation. Given the evolutionary behavior of EDE, the fundamental particle physics parameters m and f can be related to the phenomenological parameters $\log_{10}z_c$ and $f_{\rm EDE}(z_c)$. Here, $f_{\rm EDE}(z_c)$ is the maximum fraction of the total energy density in the scalar field, and z_c is the redshift at which this fraction reaches its maximum. Therefore, the EDE component is governed by three parameters: $\log_{10}z_c$, $f_{\rm EDE}(z_c)$ and the initial misalignment angle $\theta_i = \phi_i/f$, with ϕ_i being the initial field value. As shown in [7], m largely controls the value of z_c, while f controls the value of $f_{\rm EDE}(z_c)$. And the approximate equations relating m to z_c and f to $f_{\rm EDE}(z_c)$ are:

$$m^2|(1 - \cos\theta_i)^2(2 + 3\cos\theta_i)| \simeq 3H(z_c)^2\,, \quad (2.6)$$

$$f_{\rm EDE}(z_c) \simeq \frac{m^2f^2}{\rho_{\rm tot}(z_c)}(1 - \cos\theta_i)^3\,. \quad (2.7)$$

It can be inferred from the above equations that for a fixed θ_i, a value of m determines z_c and a value of f determines $f_{\rm EDE}(z_c)$. According to [71], θ_i, once other EDE parameters are fixed, is a parameter whose value controls the oscillation frequency of the background field. It is tightly constrained by the small-scale polarization measurements: in fact, the full Planck 2015 dataset, excluding the region $\theta_i < 1.8$ at 95% confidence level.

The evolution of the energy density of WDM, however, is described by a simpler equation, namely, the continuity equation of WDM:

$$\dot{\rho}_{\rm dm} + 3H(1 + w_{\rm dm})\rho_{\rm dm} = 0. \tag{2.8}$$

Here, $w_{\rm dm}$ is the EoS of WDM, and it is a constant. After solving this equation, we obtain $\rho_{\rm dm} = \rho_{\rm dm0}a^{-3(1+w_{\rm dm})}$ (without losing any generality, we set the current value of the scale factor a_0 to be unity). According to this formula, WDM dilutes either faster or slower than CDM, depending on the sign of $w_{\rm dm}$.

The EDE+WDM model is determined by ten parameters: six basic parameters shared with ΛCDM, plus four new parameters, namely, $\log_{10} z_c$, $f_{\rm EDE}(z_c)$, θ_i and $w_{\rm dm}$.

At the linear perturbation level, the perturbation of the scalar field ϕ (in the Fourier space) is governed by the linearized KG equation:

$$\delta\phi_k'' + 2\mathcal{H}\delta\phi_k' + (k^2 + a^2V_{,\phi\phi})\delta\phi_k = -h'\phi'/2 \tag{2.9}$$

where the prime denotes the derivative with respect to conformal time, $\mathcal{H}$ is the conformal Hubble parameter, h is the metric potential in synchronous gauge and k is the magnitude of the wavenumber $\vec{k}$.

On the other hand, the linear perturbation equations of WDM consist of the continuity and Euler equations of this component, i.e.:

$$\delta_{\rm dm}' = -(1 + w_{\rm dm})\left(\theta_{\rm dm} + \frac{1}{2}h'\right) - 3\mathcal{H}\delta_{\rm dm}(c_{\rm s,dm}^2 - w_{\rm dm}) - 9(1 + w_{\rm dm})(c_{\rm s,dm}^2 - c_{\rm a,dm}^2)\mathcal{H}^2\frac{\theta_{\rm dm}}{k^2}, \tag{2.10}$$

$$\theta_{\rm dm}' = -(1 - 3c_{\rm s,dm}^2)\mathcal{H}\theta_{\rm dm} + \frac{c_{\rm s,dm}^2}{1 + w_{\rm dm}}k^2\delta_{\rm dm}, \tag{2.11}$$

where $\delta_{\rm dm}$ and $\theta_{\rm dm}$ are the relative density and velocity divergence perturbations of DM, and $c_{\rm s,dm}$ and $c_{\rm a,dm} = \dot{p}_{\rm dm}/\dot{\rho}_{\rm dm}$ denote the sound speed and adiabatic sound speed of DM. The sound speed of DM describes its micro-scale properties and needs to be provided independently; in this article, we consider $c_{\rm s,dm}^2 = 0$ to understand the extent to which modifying the DM EoS alone can alleviate the S_8 tension. Having presented the equations above, the background and perturbation dynamics of the EDE+WDM model are clearly understood.

At the end of this section, we present some implications regarding the impacts of EDE+WDM on the CMB TT and matter power spectra. For a simplified demonstration of these effects, we display, in figure 1, the CMB TT and matter power spectra of EDE+WDM, along with their residuals compared to a baseline ΛCDM model. We define our benchmark ΛCDM model with the following cosmological parameters: the peak scale parameter $100\theta_s = 1.041783$, the baryon density today $\omega_b = 0.02238280$, the DM density today $\omega_{\rm dm} = 0.1201705$, the optical depth $\tau_{\rm reio} = 0.0543082$, the amplitude of the primordial scalar $A_s = 2.100549 \times 10^{-9}$, and the spectral index of the primordial scalar $n_s = 0.9660499$. These values are extracted from the Planck 2018 + lowE + lensing dataset [2]. The six basic parameters of EDE+WDM are fixed to the values of their counterparts in the baseline ΛCDM model. Other parameters, namely, $\log_{10} z_c$, $f_{\rm EDE}(z_c)$, θ_i and $w_{\rm dm}$, are set to the following values for different choices: 3.5, 0, 2.5, 0.001; 3.5, 0, 2.5, 0; 3.5, 0, 2.5, −0.001; and 3.5, 0.05, 2.5, 0. Of course, we point out that the values of six basic parameters of EDE+WDM extracted from the Planck 2018 + lowE + lensing dataset are different from the six corresponding values provided above. In fact, EDE+WDM has a larger value of $\omega_{\rm cdm}$ compared to ΛCDM due to the $w_{\rm dm}$-$\omega_{\rm dm}$ and EDE-$\omega_{\rm dm}$ degeneracy, and this will lead to different CMB TT and matter power spectra. However, to consider the individual impact of changing the values of $w_{\rm dm}$ and $f_{\rm EDE}(z_c)$ on the CMB TT and matter power spectra, we set the values of the six basic parameters for both EDE+WDM and ΛCDM to be consistent.

Focusing on the CMB TT power spectrum and fixing the $f_{\rm EDE}(z_c)$ parameter, we observe that the amplitudes of the acoustic peaks in the CMB predicted by EDE+WDM with a negative $w_{\rm dm}$ are increased. This is attributed to the fact that negative values of the parameter $w_{\rm dm}$ will postpone the moment of matter–radiation equality when other model parameters are fixed. On larger scales where $l < 10$, the curves are depressed when the value of the parameter $w_{\rm dm}$ is negative due to the integrated Sachs–Wolfe effect. In addition, when the values of the parameter $w_{\rm dm}$ turn positive, while keeping the values of other relevant cosmological parameters unchanged, the resulting effects are opposite to those observed with negative values of $w_{\rm dm}$. On the other hand, when fixing the $w_{\rm dm}$ parameter, an increase in the amplitudes of the acoustic peaks in the CMB is observed in EDE+WDM when $f_{\rm EDE}(z_c)$ is non-zero. Additionally, the curves show an increase on larger scales under these circumstances. These effects differ from those arising from a positive or negative $w_{\rm dm}$.

Concentrating on the matter power spectrum with a fixed $f_{\rm EDE}(z_c)$ parameter, it becomes evident that a negative value of $w_{\rm dm}$ results in a decrease, while positive values of $w_{\rm dm}$ lead to an increase in the matter power spectrum; this is because the former situation results in a delay of matter and radiation equality, while the latter situation leads to an advance of matter and radiation equality. However, when fixing the $w_{\rm dm}$ parameter, a non-zero value of $f_{\rm EDE}(z_c)$ leads to a different outcome, i.e. an increase in the large scale and a decrease in the small scale of the matter power spectrum. From these effects, one can infer that a non-zero $f_{\rm EDE}(z_c)$ itself is not the direct reason for the worsening S_8 tension, considering it leads to a decrease in the small scale of the power spectrum. The

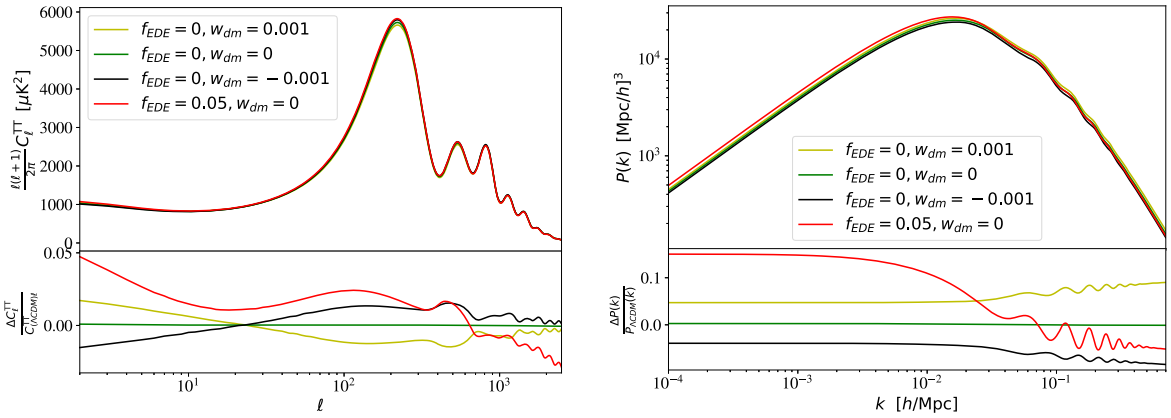

Figure 1. The CMB TT and matter power spectra are computed for different values of the parameters $f_{\rm EDE}(z_c)$ and $w_{\rm dm}$, while keeping six basic parameters fixed at the values of their counterparts in the baseline ΛCDM model, as extracted from the Planck 2018 + lowE + lensing data. Additionally, $\log_{10} z_c$ and θ_i are set to 3.5 and 2.5.

problem arises from the EDE-$\omega_{\rm dm}$ degeneracy; it counteracts the effects of a non-zero $f_{\rm EDE}(z_c)$, and we hope that a negative $w_{\rm dm}$, in addition to a non-zero $f_{\rm EDE}(z_c)$, will solve this problem[3].

3. Datasets and methodology

To extract the mean values and confidence intervals of the model parameters, we utilize the recent observational datasets described below.

Cosmic microwave background (**CMB**): we make use of the Planck 2018 [2, 72, 73] CMB temperature, polarization and lensing measurements that include plik TTTEEE, lowl, lowE and the lensing likelihood.

Baryon acoustic oscillations (**BAO**): we also utilize several BAO distance measurements, including 6dFGS [74], SDSS-MGS [75] and BOSS DR12 [76].

Pantheon: the Pantheon catalogue of Supernovae Type Ia, comprising 1048 data points in the redshift region $z \in [0.01, 2.3]$, is also considered.

Hubble constant: the latest local measurements of the Hubble constant obtained by Riess *et al* [1], i.e. $H_0 = 73.04 \pm 1.04$ are also included; we denote it as R22 hereafter.

S_8 parameter: in addition to the above datasets, we include a Gaussianized prior on S_8, i.e. $S_8 = 0.766 \pm 0.017$, chosen according to the joint analysis of KID1000+BOSS +2dLenS. (The use of a prior as an approximation for the full WL likelihoods has been demonstrated to be justified in the context of EDE models [77]. Nevertheless, in the EDE +WDM model, a comprehensive assessment of the likelihoods necessitates dedicated treatment of nonlinearities. Due to the absence of such tools, we restrict our analysis to the linear power spectrum, and make the assumption that the incorporation of this S_8 prior correctly captures the constraints from the KID1000+BOSS+2dLenS likelihoods on EDE+WDM.)

To constrain the EDE+WDM model, we run a Markov Chain Monte Carlo using the public code MontePython-v3 [78, 79], interfaced with a modified version of the CLASS_EDE code [77], which is an extension to the CLASS code [80, 81]. We perform the analysis with a Metropolis–Hastings algorithm and consider chains to be converged using the Gelman–Rubin [82] criterion $R - 1 < 0.03$, assuming flat priors in the following parameter space:

$$\mathcal{P} = \{\omega_b,\ \omega_{\rm dm},\ \theta_s,\ A_s,\ n_s,\ \tau_{\rm reio},\ \log_{10} z_c,\ f_{\rm EDE}(z_c),\ \theta_i,\ w_{\rm dm}\}. \tag{3.1}$$

We also adopt the Planck collaboration convention and model free-streaming neutrinos as two massless species and one massive with $M_\nu = 0.06$ eV.

4. Results and discussion

In this section we constrain EDE+WDM, EDE[4], ΛWDM and ΛCDM using CMB, BAO and Pantheon datasets, as well as R22 and the Gaussianized prior on S_8 that we showed in the previous section in order to perform a statistical comparison between these models with the aim to focus on the tension on both H_0 and S_8.

In table 1, we present the observational constraints on EDE+WDM, EDE, ΛWDM and ΛCDM based on the CMB+BAO+Pantheon+H_0+S_8 dataset. Figure 2 shows the one-dimensional posterior distributions and two-dimensional joint contours at 68% and 95% confidence levels for the most relevant parameters of EDE+WDM, EDE, ΛWDM and ΛCDM. From table 1, one can see that the values of parameters $w_{\rm dm}$ of both EDE+WDM and ΛWDM are very close to 0. This does not come as a surprise, since otherwise the LSS cannot be correctly formed. In addition, we find that the

[3] It is worth mentioning that, if both the values of $w_{\rm dm}$ and $f_{\rm EDE}(z_c)$ are non-zero, then it is not difficult to infer that, as long as both values are small enough, the observed results in the power spectrum will be a combination of the outcomes corresponding to only one of the two values being zero.

[4] 'EDE' here represents the axion-like early dark energy model instead of early dark energy; the specific meaning of 'EDE' will no longer be explicitly stated in the following content. Readers are encouraged to infer its significance based on the context.

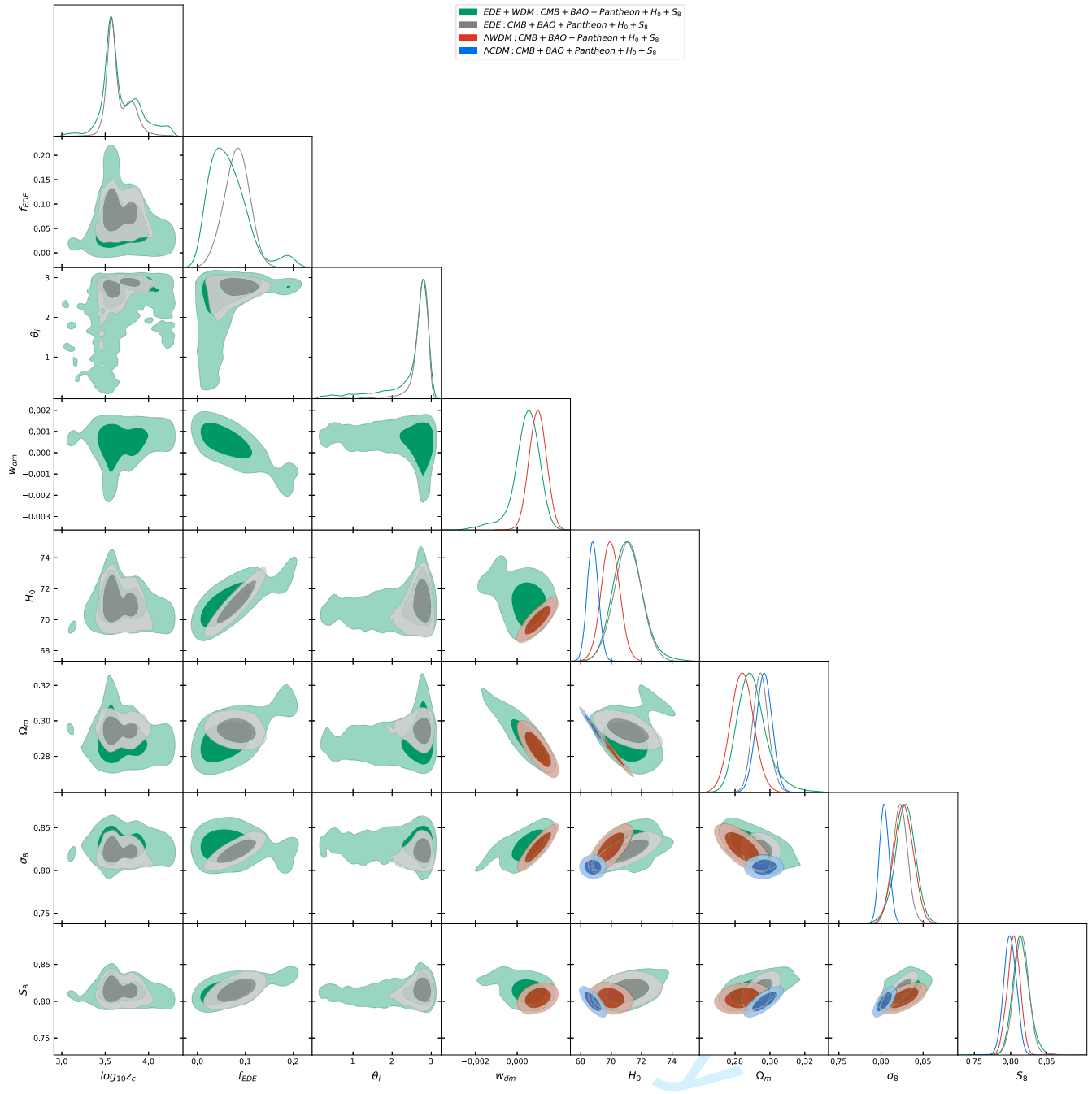

Figure 2. One-dimensional posterior distributions and two-dimensional joint contours at 68% and 95% confidence levels for the most relevant parameters of EDE+WDM, EDE, ΛWDM and ΛCDM are presented using the CMB+BAO+Pantheon+H_0+S_8 dataset.

fitting results for the H_0 parameter in EDE+WDM, i.e. $71.11^{+0.88}_{-1.0}$ at 68% confidence level, are similar to that of EDE, i.e. 71.10 ± 0.90 at 68% confidence level. It still maintains the ability to alleviate the Hubble tension to $\sim$1.4 σ, which is a notable improvement compared to that of ΛWDM, i.e. 69.95 ± 0.60 at 68% confidence level (with Hubble tension $\sim$2.6 σ) and that of ΛCDM, i.e. 68.79 ± 0.37 at 68% confidence level (with Hubble tension $\sim$3.9 σ). However, unfortunately, we find that the fitting result for the S_8 parameter in EDE+WDM, i.e. $0.814^{+0.011}_{-0.012}$ at 68% confidence level, is also similar to that of EDE, i.e. 0.815 ± 0.011 at 68% confidence level, showing a $\sim$2.3 σ tension on the S_8 parameter, which is still worse than that of ΛWDM, i.e. $S_8 = 0.8043^{+0.0093}_{-0.0084}$ 68% confidence level (with S_8 tension $\sim$2 σ) and that of ΛCDM, i.e. $S_8 = 0.7994 \pm 0.0086$ 68% confidence level (with S_8 tension $\sim$1.8 σ). We attribute the failure of the EDE+WDM model to alleviate the S_8 tension to the lack of a positive(negative) correlation between the S_8 parameter and the $w_{\rm dm}$ parameter, as well as a sufficiently large negative(positive) value of $w_{\rm dm}$ in this model. Although, as expected, there is a positive correlation between the $w_{\rm dm}$ parameter and the σ_8 parameter in this model, the negative

Table 1. The mean values and 1, 2 σ errors of the parameters for EDE+WDM, EDE, ΛWDM and ΛCDM are provided for the CMB+BAO+Pantheon+S_8+H_0 dataset, along with the AIC values for these four models.

Model	ΛCDM	ΛWDM	EDE	EDE+WDM
Dataset	CMB + BAO + Pantheon + S_8 + H_0			
$100\,\omega_b$	$2.265 \pm 0.013^{+0.025}_{-0.025}$	$2.248 \pm 0.014^{+0.027}_{-0.027}$	$2.286 \pm 0.021^{+0.041}_{-0.040}$	$2.274 \pm 0.024^{+0.048}_{-0.045}$
$\omega_{\rm cdm}$	$0.11707 \pm 0.000\,81^{+0.0016}_{-0.0016}$	$0.11586 \pm 0.000\,89^{+0.0018}_{-0.0017}$	$0.1255 \pm 0.0033^{+0.0063}_{-0.0062}$	$0.1233^{+0.0027}_{-0.0060}{}^{+0.020}_{-0.0088}$
$100\,\theta_s$	$1.04218 \pm 0.000\,29^{+0.00055}_{-0.00058}$	$1.04202 \pm 0.000\,28^{+0.00055}_{-0.00056}$	$1.04163 \pm 0.000\,38^{+0.00071}_{-0.00073}$	$1.04163^{+0.00042}_{-0.00031}{}^{+0.00082}_{-0.0012}$
$\ln(10^{10}A_s)$	$3.050 \pm 0.015^{+0.030}_{-0.028}$	$3.045 \pm 0.014^{+0.028}_{-0.028}$	$3.057 \pm 0.015^{+0.029}_{-0.029}$	$3.053 \pm 0.015^{+0.032}_{-0.030}$
n_s	$0.9725 \pm 0.0037^{+0.0071}_{-0.0072}$	$0.9701 \pm 0.0036^{+0.0071}_{-0.0072}$	$0.9859 \pm 0.0065^{+0.013}_{-0.013}$	$0.9818^{+0.0068}_{-0.010}{}^{+0.022}_{-0.018}$
$\tau_{\rm reio}$	$0.0598 \pm 0.0075^{+0.016}_{-0.014}$	$0.0551^{+0.0066}_{-0.0075}{}^{+0.015}_{-0.014}$	$0.0571 \pm 0.0075^{+0.015}_{-0.015}$	$0.0556 \pm 0.0073^{+0.015}_{-0.014}$
$\log_{10} z_c$	—	—	$3.65 \pm 0.14^{+0.29}_{-0.22}$	$3.67 \pm 0.22^{+0.54}_{-0.37}$
$f_{\rm EDE}(z_c)$	—	—	$0.082^{+0.028}_{-0.025}{}^{+0.049}_{-0.054}$	$0.066^{+0.025}_{-0.047}{}^{+0.13}_{-0.071}$
θ_i	—	—	$2.71^{+0.23}_{-0.069}{}^{+0.34}_{-0.47}$	$2.48^{+0.53}_{+0.027}{}^{+0.62}_{-1.6}$
$w_{\rm dm}$	—	$0.00098 \pm 0.000\,41^{+0.00079}_{-0.00079}$	–	$0.00042^{+0.00069}_{-0.00043}{}^{+0.0013}_{-0.0014}$
H_0	$68.79 \pm 0.37^{+0.73}_{-0.70}$	$69.95 \pm 0.60^{+1.2}_{-1.2}$	$71.10 \pm 0.90^{+1.8}_{-1.8}$	$71.11^{+0.88}_{-1.0}{}^{+1.9}_{-1.9}$
Ω_m	$0.2966 \pm 0.0046^{+0.0090}_{-0.0091}$	$0.2841 \pm 0.0065^{+0.013}_{-0.013}$	$0.2948^{+0.0042}_{-0.0048}{}^{+0.0096}_{-0.0087}$	$0.2901^{+0.0064}_{-0.0097}{}^{+0.019}_{-0.016}$
σ_8	$0.8039 \pm 0.0057^{+0.011}_{-0.011}$	$0.827 \pm 0.011^{+0.022}_{-0.023}$	$0.8224 \pm 0.0094^{+0.018}_{-0.018}$	$0.828 \pm 0.014^{+0.025}_{-0.026}$
S_8	$0.7994 \pm 0.0086^{+0.017}_{-0.017}$	$0.8043^{+0.0093}_{-0.0084}{}^{+0.017}_{-0.017}$	$0.815 \pm 0.011^{+0.021}_{-0.021}$	$0.814^{+0.011}_{-0.012}{}^{+0.025}_{-0.022}$
$\chi^2_{\rm min}$	3840.76	3834.62	3827.58	3827.56
$\Delta\chi^2_{\rm min}$	0	−6.14	−13.18	−13.20
k	28	29	31	32
AIC	3896.76	3892.62	3889.58	3891.56
ΔAIC	0	−4.14	−7.18	−5.2

correlation between the $w_{\rm dm}$ parameter and Ω_m leads to the lack of correlation between the S_8 parameter and the $w_{\rm dm}$ parameter. This is somewhat different from the situation in ΛWDM. Although in ΛWDM, the $w_{\rm dm}$ parameter is also positively correlated with the σ_8 parameter while being negatively correlated with the Ω_m parameter, it still results in a slight positive correlation between the $w_{\rm dm}$ parameter and the S_8 parameter. We note that even though there is a slight positive correlation between the $w_{\rm dm}$ parameter and the S_8 parameter in the ΛWDM case, such a model still exacerbates the S_8 tension compared to ΛCDM due to the positive value of $w_{\rm dm}$. To visually illustrate the tension among the fitting results of EDE+WDM, EDE, ΛWDM, ΛCDM and the two priors included in the datasets (R22 and the Gaussianized prior on S_8), figure 3 reproduces the S_8-H_0 contours, incorporating the boundaries corresponding to one standard deviation for these two priors. It is worth mentioning that the above result is still obtained when using both H_0 prior and S_8 prior simultaneously. If we were to use only one of these priors, or none at all, the EDE+WDM model would face even greater Hubble and S_8 tensions.

We also consider the Akaike information criterion (AIC) for model comparison among the EDE+WDM, EDE, ΛWDM and ΛCDM models. The AIC is defined as $\chi^2_{\rm min} + 2k$, where k denotes the number of cosmological parameters. In practice, we are primarily interested in the relative values of AIC between two different models, denoted as $\Delta{\rm AIC} = \Delta\chi^2_{\rm min} + 2\Delta k$. A model with a smaller AIC value is considered to be more favorable. In this work, the ΛCDM model serves as the reference model. From table 1,

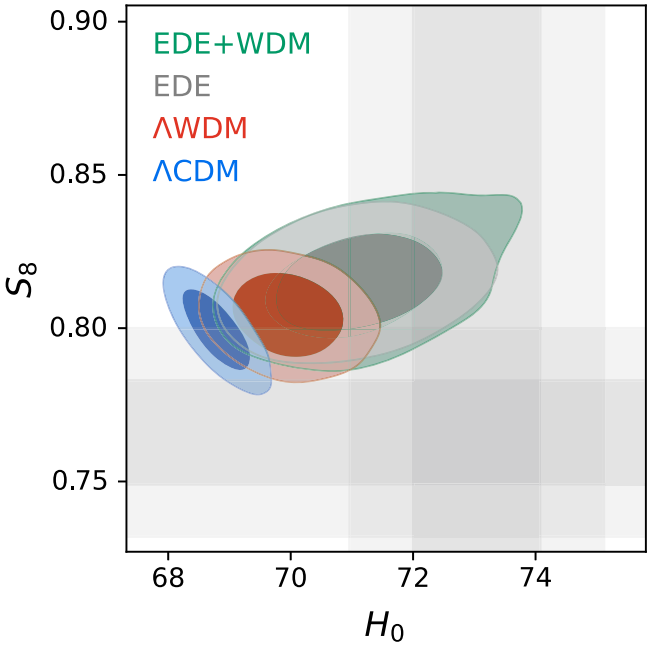

Figure 3. The S_8-H_0 contours at 68% and 95% confidence levels for EDE+WDM, EDE, ΛWDM and ΛCDM regarding the CMB+BAO +Pantheon+H_0+S_8 dataset, as well as the boundaries corresponding to one standard deviation for R22 and the Gaussianized prior.

we find that the ΔAIC values for EDE+WDM, EDE and ΛWDM are −5.2, −7.18 and −4.14, respectively. Therefore, for the CMB+BAO+Pantheon+H_0+S_8 dataset, EDE is the most favorable model among the four models analyzed in this work.

Generally speaking, the observational data forces the $w_{\rm dm}$ of EDE+WDM to be very close to 0, resulting in EDE +WDM not differing much from EDE. Additionally, a negative $w_{\rm dm}$ lacks a common physical explanation. Also, as shown above, EDE+WDM is not favored by the observational data compared to EDE, as its AIC is worse than that of EDE. Furthermore, EDE+WDM cannot alleviate the Hubble tension and the S_8 tension. In short, adding a new degree of freedom $w_{\rm dm}$ is not a good choice.

5. Concluding remarks

The Hubble tension remains a complex issue in cosmology. The current consensus within the scientific community suggests that, if systematics are not the origin of the Hubble tension, modifications are necessary both in the early and late stages compared to ΛCDM [19]. Early-time modifications are deemed necessary to simultaneously increase the Hubble constant and reduce the sound horizon. However, such modifications fail to address the Hubble tension without exacerbating other tensions, such as the S_8 tension. One of the most prominent early-time solutions is the axion-like EDE model, which considers a non-zero EDE fraction $f_{\rm EDE}(z_c)$ near the matter–radiation equality. This increases the DM density and exacerbates the S_8 tension. Given that the axion-like EDE model is a typical early-time solution and a negative DM EoS is conducive to reduce the value of the σ_8 parameter, we extend the axion-like EDE model by replacing the CDM in this model with DM characterized by a constant EoS $w_{\rm dm}$. We then impose constraints on this axion-like EDE extension model, i.e. EDE+WDM, along with three other models: the axion-like EDE model, i.e. EDE, ΛWDM and ΛCDM. These constraints are extracted from a comprehensive analysis incorporating data from the Planck 2018 CMB, BAO and the Pantheon compilation, as well as R22 and the Gaussianized prior on S_8 determined through the joint analysis of KID1000 +BOSS+2dLenS. Our findings indicate that, while EDE +WDM maintains EDE's ability to alleviate the Hubble tension to $\sim 1.4\sigma$, it still moderately exacerbates the S_8 tension. In fact, a non-zero DM EoS not only affects the value of σ_8 but also shifts the value of Ω_m; the combination of these two effects leads to the value of S_8 remaining close to that of the CDM case. Finally, we employ AIC to make a model comparison between EDE+WDM, EDE, ΛWDM and ΛCDM regarding the CMB+BAO+Pantheon+H_0+S_8 dataset. Our analysis reveals that the EDE model is the most supported model among these four models regarding this dataset. Since EDE+WDM is not favored by the observational data compared to EDE, and EDE+WDM cannot alleviate both the Hubble tension and the S_8 tension, we conclude that adding a new degree of freedom $w_{\rm dm}$ is not a good choice.

Acknowledgments

This work is supported by the National Key R&D Program of China (Grant No. 2020YFC2201600), the National Natural Science Foundation of China (NSFC) under Grant No. 12 073 088, and the National SKA Program of China No. 2020SKA0110402.

References

[1] Riess A G *et al* 2022 A comprehensive measurement of the local value of the Hubble constant with 1 $km \cdot s^{-1} \cdot Mpc^{-1}$ uncertainty from the Hubble space telescope and the SH0ES team *Astrophys. J. Lett.* **934** L7
[2] Aghanim N *et al* 2020 Planck 2018 results-VI. Cosmological parameters *Astron. Astrophys.* **641** A6
[3] Poulin V, Smith T L, Karwal T and Kamionkowski M 2019 Early dark energy can resolve the Hubble tension *Phys. Rev. Lett.* **122** 221301
[4] Agrawal P, Cyr-Racine F-Y, Pinner D and Randall L 2019 Rock'n'roll solutions to the Hubble tension arXiv:1904.01016
[5] Lin M-X, Benevento G, Hu W and Raveri M 2019 Acoustic dark energy: potential conversion of the Hubble tension *Phys. Rev.* D **100** 063542
[6] Ye G and Piao Y-S 2020 Is the Hubble tension a hint of ADS phase around recombination? *Phys. Rev.* D **101** 083507
[7] Smith T L, Poulin V and Amin M A 2020 Oscillating scalar fields and the Hubble tension: a resolution with novel signatures *Phys. Rev.* D **101** 063523
[8] Akarsu Ö, Barrow J D, Escamilla L A and Vazquez J A 2020 Graduated dark energy: observational hints of a spontaneous sign switch in the cosmological constant *Phys. Rev.* D **101** 063528
[9] Braglia M, Emond W T, Finelli F, Gümrükçüoğlu A E and Koyama K 2020 Unified framework for early dark energy from α-attractors *Phys. Rev.* D **102** 083513
[10] Vagnozzi S 2021 Consistency tests of ΛCDM from the early integrated Sachs–Wolfe effect: implications for early-time new physics and the Hubble tension *Phys. Rev.* D **104** 063524
[11] Niedermann F and Sloth M S 2021 New early dark energy *Phys. Rev.* D **103** L041303
[12] Freese K and Winkler M W 2021 Chain early dark energy: a proposal for solving the Hubble tension and explaining todays dark energy *Phys. Rev.* D **104** 083533
[13] Battye R A and Moss A 2014 Evidence for massive neutrinos from cosmic microwave background and lensing observations *Phys. Rev. Lett.* **112** 051303
[14] Zhang J-F, Geng J-J and Zhang X 2014 Neutrinos and dark energy after Planck and BICEP2: data consistency tests and cosmological parameter constraints *J. Cosmol. Astropart. Phys.* **2014** 044
[15] Zhang J, Li Y and Zhang X 2015 Sterile neutrinos help reconcile the observational results of primordial gravitational waves from Planck and BICEP2 *Phys. Lett.* B **740** 359
[16] Feng L, Zhang J and Zhang X 2018 Searching for sterile neutrinos in dynamical dark energy cosmologies *Sci. Chinaphys. Mech. Astron.* **61** 050411
[17] Zhao M, Zhang J and Zhang X 2018 Measuring growth index in a universe with massive neutrinos: a revisit of the general relativity test with the latest observations *Phys. Lett.* B **779** 473

[18] Choudhury S R and Choubey S 2019 Constraining light sterile neutrino mass with the BICEP2/Keck Array 2014 B-mode polarization data *Eur. Phys. J.* C **79** 557
[19] Vagnozzi S 2023 Seven hints that early-time new physics alone is not sufficient to solve the Hubble tension *Universe* **9** 393
[20] Huang Q-G and Wang K 2016 How the dark energy can reconcile Planck with local determination of the Hubble constant *Eur. Phys. J.*C **76** 1
[21] Vagnozzi S, Dhawan S, Gerbino M, Freese K, Goobar A and Mena O 2018 Constraints on the sum of the neutrino masses in dynamical dark energy models with $w(z) \geqslant -1$ are tighter than those obtained in ΛCDM *Phys. Rev.* D **98** 083501
[22] Martinelli M and Tutusaus I 2019 CMB tensions with low-redshift H_0 and S_8 measurements: impact of a redshift-dependent type-Ia supernovae intrinsic luminosity *Symmetry* **11** 986
[23] Visinelli L, Vagnozzi S and Danielsson U 2019 Revisiting a negative cosmological constant from low-redshift data *Symmetry* **11** 1035
[24] Alestas G, Kazantzidis L and Perivolaropoulos L 2020 H_0 tension, phantom dark energy, and cosmological parameter degeneracies *Phys. Rev.* D **101** 123516
[25] Vagnozzi S 2020 New physics in light of the H_0 tension: an alternative view *Phys. Rev.* D **102** 023518
[26] Alestas G and Perivolaropoulos L 2021 Late-time approaches to the Hubble tension deforming H(z), worsen the growth tension *Mon. Not. R. Astron. Soc.* **504** 3956
[27] Kumar S and Nunes R C 2016 Probing the interaction between dark matter and dark energy in the presence of massive neutrinos *Phys. Rev.* D **94** 123511
[28] Kumar S and Nunes R C 2017 Echo of interactions in the dark sector *Phys. Rev.* D **96** 103511
[29] Di Valentino E, Melchiorri A and Mena O 2017 Can interacting dark energy solve the H_0 tension? *Phys. Rev.* D **96** 043503
[30] Yang W, Pan S, Di Valentino E, Nunes R C, Vagnozzi S and Mota D F 2018 Tale of stable interacting dark energy, observational signatures, and the H_0 tension *J. Cosmol. Astropart. Phys.* **2018** 019
[31] Yang W, Mukherjee A, Di Valentino E and Pan S 2018 Interacting dark energy with time varying equation of state and the H_0 tension *Phys. Rev.* D **98** 123527
[32] Kumar S, Nunes R C and Yadav S K 2019 Dark sector interaction: a remedy of the tensions between CMB and LSS data *Eur. Phys. J.* C **79** 1
[33] Yang W, Mena O, Pan S and Valentino E D 2019 Dark sectors with dynamical coupling *Phys. Rev.* D **100** 083509
[34] Yao Y-H and Meng X-H 2020 A new coupled three-form dark energy model and implications for the H_0 tension *Phys. Dark Universe* **30** 100729
[35] Di Valentino E, Melchiorri A, Mena O and Vagnozzi S 2020 Nonminimal dark sector physics and cosmological tensions *Phys. Rev.* D **101** 063502
[36] Di Valentino E, Melchiorri A, Mena O and Vagnozzi S 2020 Interacting dark energy in the early 2020s: a promising solution to the H_0 and cosmic shear tensions *Phys. Dark Universe* **30** 100666
[37] Lucca M and Hooper D C 2020 Tensions in the dark: shedding light on dark matter-dark energy interactions arXiv:2002.06127
[38] Yang W, Di Valentino E, Mena O and Pan S 2020 Dynamical dark sectors and neutrino masses and abundances *Phys. Rev.* D **102** 023535
[39] Nunes R C, Vagnozzi S, Kumar S, Di Valentino E and Mena O 2022 New tests of dark sector interactions from the full-shape galaxy power spectrum *Phys. Rev.* D **105** 123506
[40] Bernal J L, Verde L and Riess A G 2016 The trouble with H_0 *J. Cosmol. Astropart. Phys.* **2016** 019
[41] Addison G, Watts D, Bennett C, Halpern M, Hinshaw G and Weiland J 2018 Elucidating ΛCDM: impact of baryon acoustic oscillation measurements on the Hubble constant discrepancy *Astrophys. J.* **853** 119
[42] Lemos P, Lee E, Efstathiou G and Gratton S 2019 Model independent H(z) reconstruction using the cosmic inverse distance ladder *Mon. Not. R. Astron. Soc.* **483** 4803
[43] Aylor K, Joy M, Knox L, Millea M, Raghunathan S and Wu W K 2019 Sounds discordant: classical distance ladder and ΛCDM-based determinations of the cosmological sound horizon *Astrophys. J.* **874** 4
[44] Knox L and Millea M 2020 Hubble constant hunters guide *Phys. Rev.* D **101** 043533
[45] Macaulay E, Wehus I K and Eriksen H K 2013 Lower growth rate from recent redshift space distortion measurements than expected from Planck *Phys. Rev. Lett.* **111** 161301
[46] Joudaki S *et al* 2016 CHFTLenS revisited: assessing concordance with Planck including astrophysical systematics *Mon. Not. R. Astron. Soc.* **465** 2033–52
[47] Bull P *et al* 2016 Beyond ΛCDM: problems, solutions, and the road ahead *Phys. Dark Universe* **12** 56
[48] Joudaki S *et al* 2017 KIDS-450: testing extensions to the standard cosmological model *Mon. Not. R. Astron. Soc.* **471** 1259
[49] Nesseris S, Pantazis G and Perivolaropoulos L 2017 Tension and constraints on modified gravity parametrizations of $G_{eff}(z)$ from growth rate and Planck data *Phys. Rev.* D **96** 023542
[50] Kazantzidis L and Perivolaropoulos L 2018 Evolution of the fσ_8 tension with the Planck 15/ΛCDM determination and implications for modified gravity theories *Phys. Rev.* D **97** 103503
[51] Asgari M *et al* 2020 KiDS+ VIKING-450 and DES-Y1 combined: mitigating baryon feedback uncertainty with COSEBIs *Astron. Astrophys.* **634** A127
[52] Hildebrandt H *et al* 2020 KiDS+ VIKING-450: cosmic shear tomography with optical and infrared data *Astron. Astrophys.* **633** A69
[53] Skara F and Perivolaropoulos L 2020 Tension of the EG statistic and redshift space distortion data with the Planck-ΛCDM model and implications for weakening gravity *Phys. Rev.* D **101** 063521
[54] Abbott T *et al* 2020 Dark energy survey year 1 results: cosmological constraints from cluster abundances and weak lensing *Phys. Rev.* D **102** 023509
[55] Joudaki S *et al* 2020 KiDS+ VIKING-450 and DES-Y1 combined: cosmology with cosmic shear *Astron. Astrophys.* **638** L1
[56] Heymans C *et al* 2021 KIDS-1000 cosmology: multi-probe weak gravitational lensing and spectroscopic galaxy clustering constraints *Astron. Astrophys.* **646** A140
[57] Asgari M *et al* 2021 KIDS-1000 cosmology: cosmic shear constraints and comparison between two point statistics *Astron. Astrophys.* **645** A104
[58] Loureiro A *et al* 2021 KIDS & Euclid: cosmological implications of a pseudo angular power spectrum analysis of KIDS-1000 cosmic shear tomography arXiv:2110.06947
[59] Abbott T *et al* 2022 Dark energy survey year 3 results: cosmological constraints from galaxy clustering and weak lensing *Phys. Rev.* D **105** 023520
[60] Amon A *et al* 2022 Dark energy survey year 3 results: cosmology from cosmic shear and robustness to data calibration *Phys. Rev.* D **105** 023514
[61] Secco L *et al* 2022 Dark energy survey year 3 results: cosmology from cosmic shear and robustness to modeling uncertainty *Phys. Rev.* D **105** 023515
[62] Philcox O H and Ivanov M M 2022 BOSS DR12 full-shape cosmology: ΛCDM constraints from the large-scale galaxy

power spectrum and bispectrum monopole *Phys. Rev.* D **105** 043517
[63] Murgia R, Abellán G F and Poulin V 2021 Early dark energy resolution to the Hubble tension in light of weak lensing surveys and lensing anomalies *Phys. Rev.* D **103** 063502
[64] Allali I J, Hertzberg M P and Rompineve F 2021 Dark sector to restore cosmological concordance *Phys. Rev.* D **104** L081303
[65] Fondi E, Melchiorri A and Pagano L 2022 No evidence for EDE from Planck data in extended scenarios arXiv:2203.12930
[66] Karwal T, Raveri M, Jain B, Khoury J and Trodden M 2022 Chameleon early dark energy and the Hubble tension *Phys. Rev.* D **105** 063535
[67] McDonough E, Lin M-X, Hill J C, Hu W and Zhou S 2022 Early dark sector, the Hubble tension, and the swampland *Phys. Rev.* D **106** 043525
[68] Wang H and Piao Y-S 2022 A fraction of dark matter faded with early dark energy? arXiv:2209.09685
[69] Clark S J, Vattis K, Fan J and Koushiappas S M 2023 H_0 and S_8 tensions necessitate early and late time changes to ΛCDM *Phys. Rev.* D **107** 083527
[70] Reeves A, Herold L, Vagnozzi S, Sherwin B D and Ferreira E G 2023 Restoring cosmological concordance with early dark energy and massive neutrinos? *Mon. Not. R. Astron. Soc.* **520** 3688
[71] Karwal T and Kamionkowski M 2016 Early dark energy, the Hubble-parameter tension, and the string axiverse arXiv:1608.01309
[72] Aghanim N *et al* 2020 Planck 2018 results-V. CMB power spectra and likelihoods *Astron. Astrophys.* **641** A5
[73] Aghanim N *et al* 2020 Planck 2018 results-VIII. gravitational lensing *Astron. Astrophys.* **641** A8
[74] Beutler F *et al* 2011 The 6DF galaxy survey: baryon acoustic oscillations and the local Hubble constant *Mon. Not. R. Astron. Soc.* **416** 3017
[75] Ross A J, Samushia L, Howlett C, Percival W J, Burden A and Manera M 2015 The clustering of the SDSS DR7 main galaxy sample-I. a 4 percent distance measure at $z = 0.15$ *Mon. Not. R. Astron. Soc.* **449** 835
[76] Alam S *et al* 2017 The clustering of galaxies in the completed SDSS-III Baryon Oscillation Spectroscopic survey: cosmological analysis of the DR12 galaxy sample *Mon. Not. R. Astron. Soc.* **470** 2617
[77] Hill J C, McDonough E, Toomey M W and Alexander S 2020 Early dark energy does not restore cosmological concordance *Phys. Rev.* D **102** 043507
[78] Audren B, Lesgourgues J, Benabed K and Prunet S 2013 Conservative constraints on early cosmology with MONTEPYTHON *J. Cosmol. Astropart. Phys.* **2013** 001
[79] Brinckmann T and Lesgourgues J 2019 MontePython 3: boosted MCMC sampler and other features *Phys. Dark Universe* **24** 100260
[80] Lesgourgues J 2011 The cosmic linear anisotropy solving system (CLASS) I: overview arXiv:1104.2932
[81] Blas D, Lesgourgues J and Tram T 2011 The cosmic linear anisotropy solving system (CLASS). part II: approximation schemes *J. Cosmol. Astropart. Phys.* **2011** 034
[82] Gelman A and Rubin D B 1992 Inference from iterative simulation using multiple sequences *Stat. Sci.* 457